MOLECULAR AND CELLULAR BIOLOGY, Dec. 1999, p. 8469–8478 Vol. 19, No. 12
0270-7306/99/$04.00+0


# BCL-2 Is Phosphorylated and Inactivated by an ASK1/Jun N-Terminal Protein Kinase Pathway Normally Activated at $G_2$/M

KAZUHITO YAMAMOTO,[1] HIDENORI ICHIJO,[2] AND STANLEY J. KORSMEYER[1]*

*Departments of Pathology and Medicine, Harvard Medical School and Dana-Farber Cancer Institute, Boston, Massachusetts 02115,[1] and Department of Biomaterials Science, Faculty of Dentistry, Tokyo Medical and Dental University, Bunkyo-ku, Tokyo 113-8549, Japan[2]*

Received 21 July 1999/Accepted 14 September 1999

**Multiple signal transduction pathways are capable of modifying BCL-2 family members to reset susceptibility to apoptosis. We used two-dimensional peptide mapping and sequencing to identify three residues (Ser70, Ser87, and Thr69) within the unstructured loop of BCL-2 that were phosphorylated in response to microtubule-damaging agents, which also arrest cells at $G_2$/M. Changing these sites to alanine conferred more antiapoptotic activity on BCL-2 following physiologic death signals as well as paclitaxel, indicating that phosphorylation is inactivating. An examination of cycling cells enriched by elutriation for distinct phases of the cell cycle revealed that BCL-2 was phosphorylated at the $G_2$/M phase of the cell cycle. $G_2$/M-phase cells proved more susceptible to death signals, and phosphorylation of BCL-2 appeared to be responsible, as a Ser70Ala substitution restored resistance to apoptosis. We noted that ASK1 and JNK1 were normally activated at $G_2$/M phase, and JNK was capable of phosphorylating BCL-2. Expression of a series of wild-type and dominant-negative kinases indicated an ASK1/Jun N-terminal protein kinase 1 (JNK1) pathway phosphorylated BCL-2 in vivo. Moreover, the combination of dominant negative ASK1, (dnASK1), dnMKK7, and dnJNK1 inhibited paclitaxel-induced BCL-2 phosphorylation. Thus, stress response kinases phosphorylate BCL-2 during cell cycle progression as a normal physiologic process to inactivate BCL-2 at $G_2$/M.**

Programmed cell death plays an indispensable role in the development and maintenance of homeostasis within all multicellular organisms (62, 65). Genetic and molecular analysis of *Caenorhabditis elegans* to humans has indicated that the pathway of cellular suicide is highly conserved (14, 56). Although the capacity to carry out apoptosis appears to be inherent to all cells, their susceptibility varies markedly and is influenced by external and cell-autonomous events (49). Multiple steps in this process are subject to regulation, from cell surface death receptors to the BCL-2 family of proteins, to Apaf-1 and finally the caspases, which proteolytically cleave death substrates (10). Apoptosis has two predominant effector pathways, the activation of caspases and organelle dysfunction, of which mitochondrial dysfunction is best characterized (16). The BCL-2 family of proteins resides at a critical decisional point upstream to irreversible cellular damage, and the proteins focus much of their activities at the level of the mitochondria. The BCL-2 family possesses both pro- and antiapoptotic molecules, and their ratio determines, in part, the response to a death signal (44). Evidence that many of these molecules have inactive and active conformations has emerged. These transitions mediated by posttranslational modifications in response to death or survival signals are perhaps best characterized for the prodeath members.

Modifications to proapoptotic members include phosphorylation, dimerization, and proteolytic cleavage and often result in subcellular translocation. BAD belongs to a divergent "BH3 domain only" subset of the BCL-2 family, which possesses substantial sequence homology only within the BH3 amphipathic α helix (46, 69). In the presence of survival factor, BAD is inactivated by phosphorylation on two serine residues (Ser112 and Ser136) and sequestered in the cytosol bound to 14-3-3 (70). Upon factor deprivation, BAD is activated by dephosphorylation and found associated with BCL-$X_L$/BCL-2 at membrane sites including mitochondria. AKT/PKB/RAC, a Ser/Thr kinase downstream of phosphatidylinositol 3-kinase, is site specific for Ser136 of BAD (3, 11, 12). PKA is a BAD Ser112 site-specific kinase tethered to the outer mitochondrial membrane by an A-kinase anchoring protein which focuses this kinase-substrate interaction at the organelle where active BAD functions (22). Activation of the proapoptotic molecule BAX appears to involve subcellular translocation and dimerization (17, 24, 66). In viable cells, a substantial portion of BAX is monomeric and found either in the cytosol or loosely attached to membranes. Death stimuli result in the translocation of BAX to the mitochondria, where it is membrane integral and cross-linkable as a homodimer. Cytosolic BID is activated by caspase-8-mediated cleavage following tumor necrosis factor receptor 1/Fas death signals (18, 30, 34). The truncated p15 (tBID) targets mitochondria, and immunodepletion studies suggest that tBID is required for the release of cytochrome *c*. Structural insight into the active versus inactive conformation of BCL-2 family molecules has come from comparison of the three-dimensional structure of BID with that of BCL-$X_L$ (7, 38). One model posits that molecules with a buried hydrophobic face of the BH3 domain appear to be either antiapoptotic or inactive proapoptotic proteins. Active conformations can result from exposure of the BH3 domain and potentially other hydrophobic faces.

The founder of this family, antiapoptotic BCL-2, was discovered as a proto-oncogene at the chromosomal breakpoint of t(14;18)-bearing human B-cell lymphomas (1, 8, 60). BCL-2 is phosphorylated in response to multiple treatments, yet reports vary as to whether this modification activates or inactivates the molecule. BCL-2 is phosphorylated following exposure to the chemotherapeutic taxanes paclitaxel and taxotere, which pro-

* Corresponding author. Mailing address: Departments of Pathology and Medicine, Harvard Medical School and Dana-Farber Cancer Institute, One Jimmy Fund Way, Boston, MA 02115. Phone: (617) 632-6402. Fax: (617) 632-6401. E-mail: stanley_korsmeyer@dfci.harvard.edu.

mote microtubule assemblage (21). Phosphorylation appears to occur in an unstructured loop of BCL-2, as deletion of this loop eliminates paclitaxel-induced phosphorylation (5, 15, 54) and mutation of select serines reduces it (19). Deletion of this loop enhanced BCL-2 antiapoptotic ability, arguing that phosphorylation of BCL-2 inactivates the molecule. Paclitaxel binds peptides resembling the BCL-2 loop, suggesting a specific physical interaction among taxanes, microtubules, and a kinase for BCL-2 (51). However, the capacity of drugs including vincristine and vinblastine, which damage microtubules by other mechanisms, and even nocodazole to result in BCL-2 phosphorylation raises the possibility that this modification is related to a $G_2$/M cell cycle block (32, 53). In contrast, interleukin-3 (IL-3), a growth and survival factor used in another cell system, results in the phosphorylation of BCL-2 (36, 47). This phosphorylation has been proposed to be either required for antiapoptotic function (27) or needed to relax the antiproliferative effect of BCL-2 (47). Multiple kinases have been proposed to mediate the phosphorylation of BCL-2 following these varied stimuli. These include paclitaxel-activated Raf-1 (2), bryostatin-1-induced mitochondrion-localized PKCα (52), paclitaxel or vincristine-induced PKA (55), or Jun N-terminal kinase/stress-activated protein kinase (JNK/SAPK) when overexpressed or activated by paclitaxel (35, 54).

When we initiated this study, we believed it important to determine the precise sites of phosphorylation on BCL-2 induced by paclitaxel by using a combination of tryptic phosphopeptide mapping and sequencing. Three residues within the unstructured loop (Ser70, Ser87, and Thr69) were phosphorylated, and alteration of these sites to alanine conferred resistance to physiologic death signals as well as microtubule-damaging agents. We examined normal cycling cells enriched by elutriation for distinct phases of the cell cycle and found that BCL-2 is normally phosphorylated at $G_2$/M. Moreover, $G_2$/M-phase cells proved more susceptible to a Fas death signal, and a BCL-2 Ser70Ala mutant restored resistance. Examination of candidate kinases eliminated the cyclin B1-Cdc2 complex, revealing instead that the ASK1/JNK1 path was normally activated at $G_2$/M phase. Expression of ASK1/JNK1 correctly phosphorylated BCL-2 in vivo, while dominant negative forms of ASK1, MKK7, and JNK1 (dnASK1, dnMKK7, and dnJNK1) inhibited paclitaxel-induced BCL-2 phosphorylation. Thus, stress-activated kinase inactivates BCL-2 at the $G_2$/M phase during normal cell cycle progression as a physiologic process. Taxane treatment represents a convergence of $G_2$/M arrest, microtubule polymerization, and JNK activation that also phosphorylates and inactivates BCL-2.

## MATERIALS AND METHODS

**Plasmids.** Mammalian expression plasmid for human BCL-2 (hBCL-2) in pSFFV was described previously (67). To replace Ser70, Ser87, or Thr69 with Ala, a PCR-based site-directed mutagenesis kit (Stratagene) was used. The expression vectors for the wild type (WT) and mutants were constructed in pSFFV or pcDNA3. The Ser70 Ser87 double mutant and Thr69 Ser70 Ser87 triple mutant (AA/A) were constructed by subcloning. The hBCL-2-His bacterial expression vector was made by replacing the C-terminal hydrophobic region of hBCL-2 with a synthetic oligonucleotide-encoding hexahistidine tag and subcloned in pET-25(+) vector. ASK1-hemagglutinin epitope (HA) and dnASK1-HA(K709R) in pcDNA3 were described elsewhere (25). MKK4 and Flag-p38(AGF) expression vectors were provided by R. J. Davis (13). HA-JNK1 expression vector was a gift from J. S. Gutkind (9). pSRα-SEK1-K116R and pSRα-JNK1-APF vectors were from G. L. Johnson (28). Plasmid pMT3-HA-p38 was a gift from J. Kyriakis (50). pSRα-MKK7 and pSRα-MKK7KL expression vectors were provided by E. Nishida (41). Bacterial glutathione *S*-transferase (GST)–MKK6(K/A) expression vector was kindly provided by H. Saito (58).

**Stable transfections.** Jurkat human T cells or WEHI-231 murine B cells were cultured in RPMI 1640 supplemented with 10% fetal bovine serum (FBS), 10 mM HEPES, 50 μM 2-mercaptoethanol, L-glutamine, penicillin, and streptomycin. WEHI-231JM cells were kindly provided by C. B. Thompson (5). Transfections with various constructs in pSFFV-neo were performed by electroporation of 20 μg of linearized plasmid into $10^7$ cells at 950 μF and 200 V. After 48 h, selection with 1 mg of G418 per ml was started in 96-well plates. Neomycin (Neo)-resistant single-cell-originated clones were selected after 14 days.

**Transient transfection assay.** 293 cells were maintained in Iscove's modified Dulbecco's medium (GIBCO BRL) supplemented with 10% FBS, penicillin, and streptomycin. 293 cells grown in six-well dishes were transfected with the appropriate combinations of expression plasmids, using 8 μl of LipofectAMINE (GIBCO BRL). The total amount of plasmid DNA was kept at 1.75 μg by adding empty vector pcDNA3. Cells were harvested 24 h after transfection and, where indicated, treated with 1 μM paclitaxel for 8 h. The cell lysates were subjected to Western blot analysis.

**Western blot analysis.** Cells were lysed in 50 mM Tris (pH 7.5)–150 mM NaCl–2 mM EDTA–1 mM EGTA–1% Triton X-100 containing proteinase inhibitors (1 mM phenylmethylsulfonyl fluoride [PMSF], 2 μg of aprotinin per ml, and 2 μg of leupeptin per ml) and phosphatase inhibitors (50 mM NaF and 1 mM sodium orthovanadate), and cellular debris was removed by centrifugation at 14,000 × *g*. Samples were separated by sodium dodecyl sulfate-polyacrylamide gel electrophoresis (SDS-PAGE) and transferred to a membrane. After blocking of the membrane with 3% milk and 2% bovine serum albumin in Dulbecco's phosphate-buffered saline (PBS) for 1 h, the membrane was incubated with primary and secondary antibodies (Abs) for 1 h each and developed with enhanced chemiluminescence (Amersham). Anti-hBCL-2 Abs 6C8 and Bcl-2/100 (Pharmingen) were used at 1 μg/ml, anti-HA Ab (12CA5; Boehringer Mannheim) was used at 2 μg/ml, anti-Flag Ab (Sigma) was used at 5 μg/ml, anti-JNK1 (C-17) and anti-SEK1/MKK4 (K-18) Abs (Santa Cruz Biotechnology) were used at 1:200, anti-human JNK1/JNK2 (G151-666) Ab (Pharmingen) was used at 1.5 μg/ml, and anti-phospho-SAPK/JNK Ab and anti-phospho-p38 mitogen-activated protein (MAP) kinase Ab (New England Biolabs) were used at 1:1,000.

**Cell viability assay.** Jurkat cells were treated with 0.001, 0.01, 0.1, or 1 μM paclitaxel (Sigma) or dimethyl sulfoxide (DMSO) (control) for 24 h, collected, and resuspended in 1 μg of propidium iodide (PI) per ml in PBS. Cell populations negative for PI measured with a FACScan (Becton Dickinson) were scored as viable. Jurkat cells were also treated with 100 ng of anti-Fas antibody CH-11 (Upstate Biotechnology) per ml, and cell viability was assayed by PI exclusion at indicated time points. WEHI-231 murine B cells were treated with the anti-immunoglobulin M (IgM) antibody BET-2 supernatant at 1:100 dilution.

**Metabolic labeling and immunoprecipitation.** Cells ($10^7$) were incubated in phosphate-free 10% FBS–RPMI 1640 medium and treated with 1 μM paclitaxel for Jurkat cells or 1 μM vincristine for WEHI-231 cells for 12 h, followed by the addition of $^{32}$P-orthophosphate at 2 mCi/ml. After 4 h of labeling, cells were washed with phosphate-free medium twice and lysed in radioimmunoprecipitation assay (RIPA) buffer (20 mM Tris [pH 7.5], 150 mM NaCl, 1% NP-40, 0.5% deoxycholic acid, 0.1% SDS, 2 mM EDTA, 1 mM EGTA) with proteinase inhibitors (1 mM PMSF, 2 μg of aprotinin per ml, and 2 μg of leupeptin per ml) and phosphatase inhibitors (50 mM NaF and 1 mM sodium orthovanadate). The lysate was spun at 14,000 × *g*, and the supernatant was cleared with protein A beads for 30 min, followed by incubation with anti-hBCL-2 Ab 6C8 at 4°C for 1.5 h. The immune complex was captured with protein A beads for 1 h, washed with RIPA buffer four times, resuspended in loading buffer, and separated by SDS-PAGE. The separated samples were transferred to a membrane and visualized by autoradiography. The same membrane was also subjected to immunoblot analysis with Ab Bcl-2/100 (Pharmingen).

**Phosphatase treatment of immunoprecipitated BCL-2.** BCL-2 was immunoprecipitated with Ab 6C8 from $5 \times 10^6$ BCL-2-expressing Jurkat (Jurkat-BCL-2) cells treated with 1 μM paclitaxel. The immune complex was incubated with 400 U of λ protein phosphatase (λPPase) in 1× λPPase (50 mM Tris [pH 7.5], 0.1 mM EDTA, 5 mM dithiothreitol, 0.01% Brij 35) with or without phosphatase inhibitors (50 mM NaF, 2 mM sodium orthovanadate, 5 mM EDTA, 5 mM EGTA) at 30°C for 30 min. The reaction was terminated by adding SDS-PAGE loading buffer and boiling for 5 min. The resultant samples were separated on an SDS–14% polyacrylamide gel and subjected to immunoblot analysis.

**Phosphoamino acid analysis and two-dimensional (2D) mapping.** Immunoprecipitated BCL-2 from $^{32}$P-labeled Jurkat-BCL-2 cells was separated by SDS-PAGE and transferred to a membrane. The portion containing phosphorylated BCL-2 was excised after autoradiography, and the membrane was washed five times with deionized water. The analysis was performed by the method described by Boyle et al. (4), with minor modification.

For phosphoamino acid analysis, the BCL-2 on Immobilon-P (Millipore) was incubated in 200 μl of 6 N HCl (Pierce) at 110°C for 90 min. After evaporation of HCl, the samples were mixed with phosphoamino acid standard (1 μg each of cold phosphoserine, phosphothreonine, and phosphotyrosine [Sigma]) in pH 1.9 buffer ($H_2O$–88% formic acid–glacial acetic acid, 897:25:78), and the mixtures were applied onto a thin-layer chromatography (TLC) plate (J. T. Baker) and separated with an HTLE-7000 electrophoresis system (CBS, Del Mar, Calif.). Electrophoresis was carried out in pH 1.9 buffer at 1,500 V for 30 min for the first-dimension separation and then in pH 3.5 buffer ($H_2O$-acetic acid-pyridine, 945:50:5) at 1,300 V for 20 min for the second-dimension separation. Positions of phosphoamino acids were determined by ninhydrin (0.25% in acetone) staining.

For 2D mapping, a nitrocellulose membrane containing each phosphorylated BCL-2 species was treated with 0.5% PVP-360 (Sigma) in 100 mM acetic acid for 30 min at 37°C and then washed with deionized water five times and twice with

50 mM $NH_4HCO_3$. The proteins on the membrane were digested with 10 μg of tosylsulfonyl phenylalanyl chloromethyl ketone (TPCK)-trypsin (Worthington Biochemicals) in 50 mM $NH_4HCO_3$ overnight at 37°C. The digestion was then carried out with another fresh 10 μg of TPCK-trypsin for an additional 2 h. Peptides were dried, washed once with deionized water, and then treated with performic acid on ice for 60 min. The resultant tryptic peptides were separated on a TLC plate in the first dimension by electrophoresis in pH 1.9 buffer at 1,000 V for 27 min at 4°C, followed by ascending chromatography in the second dimension in phospho-chromatography buffer (*n*-butanol–pyridine–acetic acid–$H_2O$, 75:50:15:60). Autoradiography was used to visualize $^{32}$P-phosphopeptides.

For double digestion with TPCK-trypsin and proline-specific endopeptidase, the tryptic peptide was incubated with 3 U of proline-specific endopeptidase (ICN Biomedicals) overnight at 37°C in 50 mM $NH_4HCO_3$ (pH 7.6) followed by an additional 2-h incubation with 1 U of fresh enzyme. The digested peptides were oxidized with performic acid and then subjected to 2D mapping as described above.

To examine the comigration of a $^{32}$P-labeled tryptic peptide with a synthetic peptide, a mixture of tryptic $^{32}$P-phosphopeptides and 20 μg of the synthetic peptide bearing the corresponding phosphoamino acid were subjected to 2D mapping. Unlabeled peptides were visualized by ninhydrin.

**Manual sequencing of $^{32}$P-phosphopeptide.** The labeled peptides were scraped and eluted in pH 1.9 buffer from TLC plates, lyophilized, and resolved in 30% acetonitrile solution containing 0.1% trifluoroacetic acid. The peptides were then conjugated to a Sequelon-AA membrane at 55°C by using a Sequelon-AA reagent kit (Millipore). Manual Edman sequencing was performed as described previously (57), with minor modification. The primary change was a 55°C cleavage temperature instead of 50°C.

**Centrifugal elutriations.** Elutriations were performed as described previously (33), with minor modification. In brief, $5 \times 10^8$ Jurkat cells were injected into a Beckman JE-6B elutriation rotor and elutriated in RPMI 1640–0.5% FBS at 30°C at a constant rotor speed (2,100 rpm) with increasing flow rates from 9 to 35 ml/min. Fractions (100 to 150 ml) were collected and analyzed by FACScan for cell cycle position, and appropriate fractions were analyzed.

**In vitro kinase assay.** For measurement of JNK1 activity in vitro, $5 \times 10^6$ Jurkat cells were lysed in a lysis buffer (25 mM HEPES [pH 7.4], 150 mM NaCl, 20 mM β-glycerophosphate, 2 mM EDTA, 2 mM EGTA, 50 mM NaF, 1 mM sodium orthovanadate, 1% Triton X-100) with proteinase inhibitors (1 mM PMSF, 2 μg of aprotinin per ml, and 2 μg of leupeptin per ml). The lysates were clarified by centrifugation and immunoprecipitated with anti-JNK antibody C-17 (Santa Cruz Biotechnology) for 2 h. The immune complex was recovered with protein A-Sepharose beads (Sigma) and washed three times with lysis buffer and twice with kinase buffer (25 mM HEPES [pH 7.4], 20 mM $MgCl_2$, 20 mM β-glycerophosphate, 0.5 mM EGTA, 0.5 mM NaF, 0.5 mM sodium orthovanadate) with 1 mM PMSF. The immune complex on beads was divided into two aliquots; one was used for a kinase assay with GST–c-Jun (79) (Santa Cruz Biotechnology) as a substrate, and the other was used for assay with hBCL-2-His as a substrate. The reaction was initiated by adding 30 μl of kinase reaction mixture (kinase buffer plus 5 μCi of [γ-$^{32}$P]ATP, 20 μM unlabeled ATP, 1 mM DTT, and 1 μg of a substrate). After 20 min of incubation at 30°C, the reactions were terminated by addition of 10 μl of 4× SDS-PAGE loading buffer boiled for 5 min. Samples were resolved by SDS-PAGE and visualized by autoradiography or phosphorimaging. One-tenth of the immune complex on beads was used for immunoblot analysis to compare amounts of immunoprecipitated JNK. To measure Cdc2 kinase activity, anti-cyclin B1 Ab GNS-1 (Pharmingen) was used.

The immune complex kinase assay for endogenous ASK1 activity has been described previously (25, 43). Anti-ASK1 antiserum (DAV) was used for immunoprecipitation. GST-MKK6 and GST-p38γKN were used for coupled kinase assay, and GST-MKK6(K/A) was used for a single-step kinase assay.

**Preparation of recombinant protein.** hBCL-2-His protein was induced in *Escherichia coli* BL21(DE3) cells by adding 1 mM isopropyl-β-D-thiogalactopyranoside and purified with Ni-nitrilotriacetic acid agarose (Qiagen) and a HiTrap Q column (Pharmacia Biotech). The preparation of GST-MKK6, GST-p38γKN, and GST-MKK6(K/A) has been described elsewhere (43, 58).

## RESULTS

**Microtubule-damaging drugs induce BCL-2 mobility shifts due to phosphorylation on serine and threonine residues.** Microtubule-damaging drugs including paclitaxel result in BCL-2 mobility shifts when assessed by SDS-PAGE and immunoblotting (Fig. 1A). To demonstrate that all of these shifts were due to phosphorylation, Jurkat-BCL-2 cells were labeled with $^{32}$P-orthophosphate, immunoprecipitated with anti-hBCL-2 Ab 6C8, and blotted to a membrane after SDS-PAGE. Three discrete bands detected by autoradiography corresponded precisely to the three mobility-shifted upper bands noted upon immunoblot development of the same membrane (Fig. 1A). Treatment of immunoprecipitated BCL-2 with λ-PPase converted the shifted mobilities to the bottom, nonphosphorylated mobility (Fig. 1B). These data confirmed that all of the BCL-2 mobility shifts could be attributed to phosphorylation, and phosphorylation could be monitored by immunoblotting.

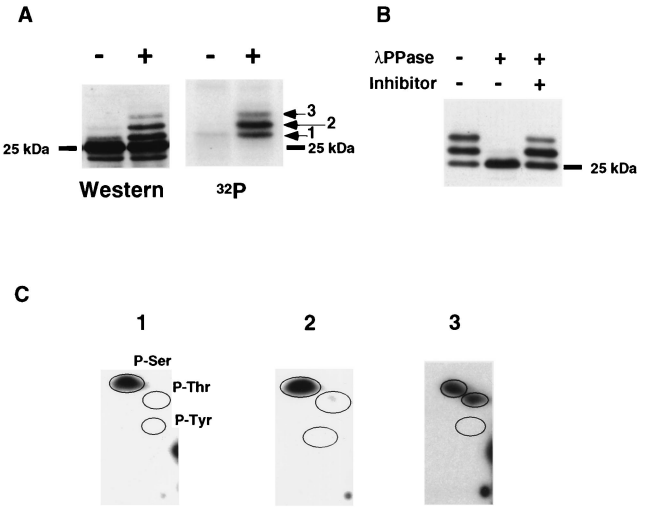


FIG. 1. BCL-2 is phosphorylated on serine and threonine in vivo. (A) The mobility shift of BCL-2 induced by paclitaxel is due to phosphorylation. BCL-2 was immunoprecipitated from $^{32}$P-orthophosphate-labeled Jurkat-BCL-2 cells treated with paclitaxel (+) or DMSO (−) by using anti-hBCL-2 Ab 6C8, separated by SDS-PAGE, and transferred to a nitrocellulose membrane. After autoradiography, the same membrane was subjected to Western analysis with anti-hBCL-2 Ab Bcl-2/100. The three $^{32}$P-labeled bands (arrows) corresponded to three mobility-shifted bands by immunoblotting. The position of nonphosphorylated BCL-2 is indicated by a dash. (B) λPPase treatment of immunoprecipitated BCL-2. Immunoprecipitated BCL-2 from Jurkat-BCL-2 cells treated with paclitaxel was incubated with λPPase at 30°C for 30 min with or without phosphatase inhibitors (50 mM NaF, 2 mM sodium orthovanadate, 5 mM EDTA, and 5 mM EGTA). The resultant samples were subjected to Western blot analysis. (C) Phosphoamino acid analysis of BCL-2. BCL-2 was immunoprecipitated from $^{32}$P-labeled Jurkat-BCL-2 cells treated with paclitaxel, separated by SDS-PAGE, and transferred to a polyvinylidene difluoride membrane. Each radioactive band on the membrane (Fig. 1A) was hydrolyzed with hydrochloric acid. The amino acid composition was determined by 2D electrophoresis on TLC plates. Encircled areas indicate the locations of phosphoserine (P-Ser), phosphothreonine (P-Thr), and phosphotyrosine (P-Tyr), visualized by ninhydrin staining; 1, 2, and 3 represent results from bands 1, 2, and 3, respectively.

To determine which amino acid residues were phosphorylated, these three bands were subjected to phosphoamino acid analysis. In bands 1 and 2, serine residues were responsible for phosphorylation (Fig. 1C), whereas band 3 was phosphorylated on threonine in addition to serine residues (Fig. 1C). Thus, paclitaxel induces BCL-2 phosphorylation on serine and threonine residues.

**Identification of Ser70, Ser87, and Thr69 in the loop region of BCL-2 as the phosphorylation sites.** Of note, the intensity of band 2 was stronger than that of band 1 by autoradiography, while their intensities were comparable by Western analysis (Fig. 1A). Moreover, the ratio of the intensity of band 3 to that of band 1 was greater by autoradiography than by immunoblotting. These observations suggested bands 2 and 3 would possess multiple phosphorylation sites. To identify the precise phosphorylation sites, 2D mapping on TLC plates and manual Edman degradation sequencing of tryptic peptides of BCL-2 were performed. Immunoprecipitated BCL-2 from a lysate of in vivo-labeled Jurkat-BCL-2 cells was separated by SDS-PAGE and blotted to a nitrocellulose membrane, and bands 1, 2, and 3 were digested with trypsin. The tryptic peptides were separated on a TLC plate according to charge and hydrophobicity. Band 1 (Fig. 1A) revealed a single spot on 2D mapping

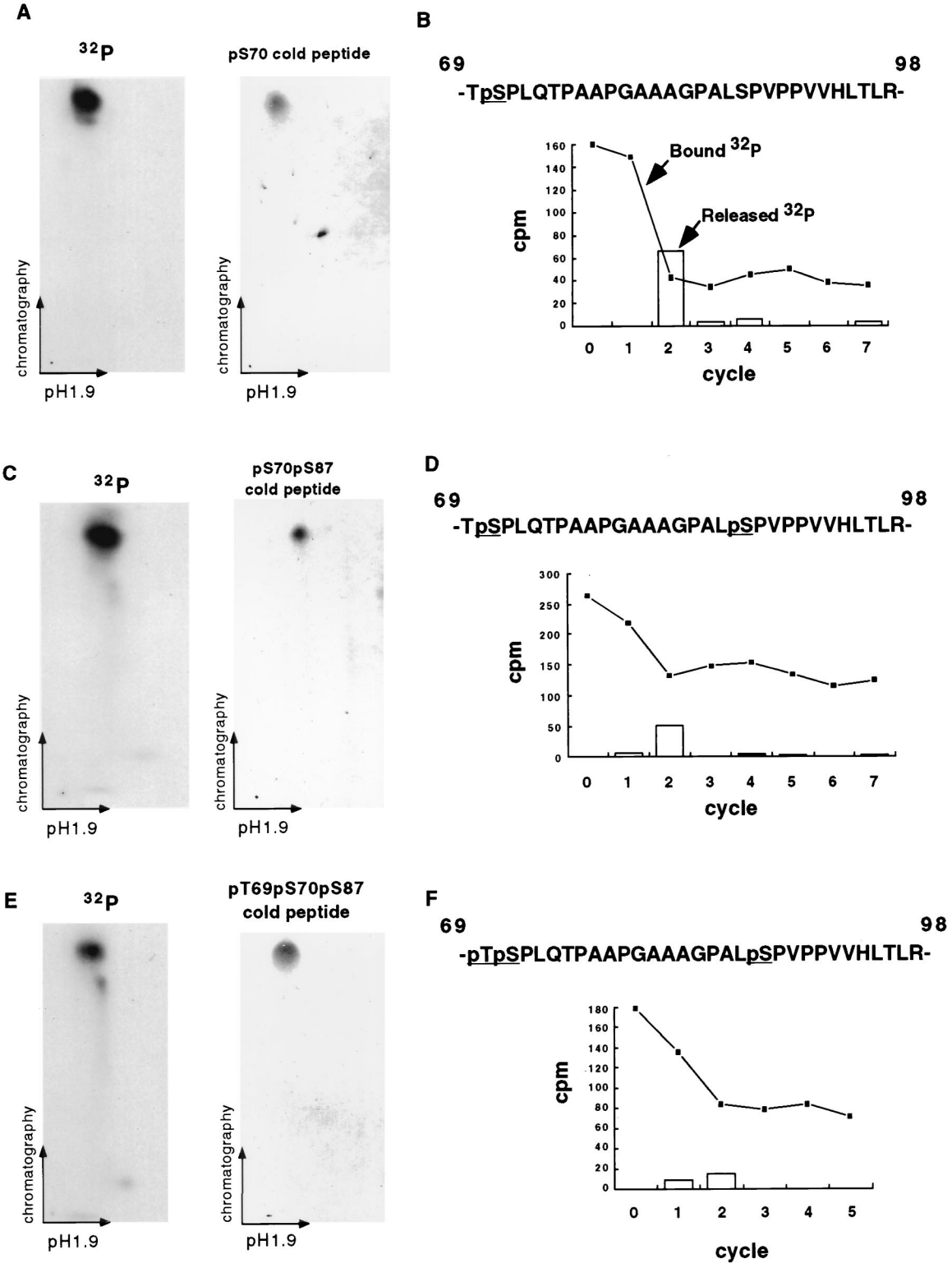


FIG. 2. Paclitaxel induces phosphorylation of Ser70, Ser87, and Thr69 in BCL-2 (A) 2D mapping and synthetic phosphopeptide comigration study of band 1. BCL-2 was immunoprecipitated from $^{32}$P-labeled Jurkat-BCL-2 cells treated with paclitaxel, size fractionated by SDS-PAGE, and transferred to a nitrocellulose membrane. The tryptic peptides of band 1 (Fig. 1A) were separated on a TLC plate by electrophoresis at pH 1.9 and chromatography. A synthetic pS70 phosphopeptide corresponding to band 1 migrated and was visualized on a TLC plate by ninhydrin staining. Moreover, the admixture of the pS70 peptide with the tryptic peptides revealed comigration on TLC plates (not shown). (B) Manual sequencing of tryptic phosphopeptide from band 1. The $^{32}$P-labeled peptide was eluted from the TLC plate, conjugated to a Sequelon-AA membrane, and subjected to manual Edman degradation. The radioactivity on the membrane (closed squares) or released into the liquid (open bars) was measured at the end of each cycle. (C and D) 2D mapping, synthetic phosphopeptide migration, and manual sequencing of band 2 as described above. (E and F) 2D mapping of synthetic phosphopeptide migration and manual sequencing of band 3 as described above. Tryptic peptides derived from bands 1, 2, and 3 were also eluted from the radioactive spots on TLC plates (A, C, and E) and subjected to phosphoamino acid analysis, confirming their composition.

(Fig. 2A) which, when subjected to manual sequencing, released the vast majority of the radioactivity, with a corresponding decrease of radioactivity bound to the membrane at the second cycle (Fig. 2B). BCL-2 possesses two tryptic peptides with a serine at position 2, located at amino acids 23 to 26 and 69 to 98. These could be distinguished because the former had no proline whereas the latter had seven. Double digestion with trypsin and proline-specific endopeptidase changed the migration of band 1 on TLC plates (data not shown), indicating that tryptic peptide 69-98 was phosphorylated and Ser70 was the phosphorylation site. The comigration of a synthetic peptide with a phospho-Ser70 confirmed this assignment (Fig. 2A).

Band 2 also revealed a single radioactive spot on 2D mapping (Fig. 2C). Manual sequencing revealed a decrease in radioactivity bound to the membrane, with corresponding release of $^{32}P$ at the second cycle (Fig. 2D). However, approximately half of the radioactivity still remained on the membrane, indicating another phosphorylation site in the same tryptic peptide. Since phosphoamino acid analysis identified only serine residues (Fig. 1C), these findings together implicated Ser87 as the second phosphorylation site. Comigration of a synthetic peptide bearing phospho-Ser70 and phospho-Ser87 confirmed the assignment of these phosphorylation sites (Fig. 2C).

2D mapping of band 3 also revealed a single radioactive spot (Fig. 2E). Manual sequencing and comigration of a phospho-Thr69-, phospho-Ser70-, and phospho-Ser87-containing synthetic peptide identified the first position, Thr69, as the third phosphorylation site (Fig. 2E and F).

To confirm these assignments and in vivo usage of phosphorylation sites, we generated Jurkat human T-cell clones and WEHI-231 murine B-cell clones expressing WT hBCL-2, alanine-substituted Ser70 (S70A) or Ser87 (S87A), or all three phosphorylation sites including Thr69 plus the two Ser residues (AA/A). Cells were labeled in vivo with $^{32}P$-orthophosphate, and BCL-2 was immunoprecipitated with anti-hBCL-2 Ab 6C8. As shown in Fig. 3A, the S70A BCL-2 now demonstrated only one phosphorylated band. The S87A BCL-2 mutant demonstrated one prominent and one faint phosphorylation band in Jurkat cells and a single band in WEHI-231 cells. The BCL-2 triple mutant (AA/A) eliminated all phosphorylation of BCL-2. Thus, the phosphorylation of BCL-2 induced by microtubule-damaging drugs was within the unstructured loop region on Ser70, Ser87, and Thr69.

**Substitution of BCL-2 phosphorylation sites results in a gain of antiapoptotic function.** To assess the relationship between BCL-2 phosphorylation and antiapoptotic function, Jurkat clones and WEHI-231 clones stably expressing comparable levels of WT BCL-2 and three BCL-2 mutants were identified (Fig. 3B). Jurkat clones were treated with a dose escalation of paclitaxel, and when assessed for viability, each clone showed dose-dependent cell death (Fig. 3C). WT BCL-2 conferred only minimal resistance compared to the Neo control (~35% versus ~28% at 1.0 μM paclitaxel). However, all three BCL-2 mutants demonstrated substantially stronger antiapoptotic function than WT BCL-2 following paclitaxel treatment. Jurkat clones expressing the three mutants S70A, S87A, and AA/A showed nearly identical enhancement of antiapoptotic function following anti-Fas Ab activation (~35 to 40% viability at 24 h) compared to WT BCL-2 (~15%) (Fig. 3D). All three mutated BCL-2 constructs were also more effective than WT BCL-2 in WEHI-231 cells treated with anti-IgM Ab (~45 to 50% versus ~30% at 72 h) (Fig. 3E). These data indicate that eliminating phosphorylation even at a single site (S87 or S70) improves antiapoptotic function of the molecule following a wide array of death stimuli.

**Endogenous BCL-2 is normally phosphorylated at $G_2$/M in cycling cells.** Since paclitaxel arrests cells at the $G_2$/M phase of the cell cycle, we asked whether its induction of BCL-2 phosphorylation might reflect an exaggerated response to a normally occurring phosphorylation of BCL-2 at $G_2$/M. To assess whether BCL-2 is normally phosphorylated throughout the cell cycle, we examined the endogenous BCL-2 within Jurkat cells enriched for specific cell cycle stages by centrifugal elutriation. Elutriation-enriched $G_1$-, S-, and $G_2$/M-phase cells from asynchronously growing Jurkat T cells were assessed for BCL-2 phosphorylation. A mobility-shifted band typical of phosphorylation was prominent in the $G_2$/M-phase population but much less intense in S phase and was not visible in $G_1$-phase cells (Fig. 4A).

**Ser70 is the principal site normally phosphorylated during the cell cycle.** Endogenous BCL-2 from the $G_2$/M-enriched fraction of Jurkat cells displayed only a single mobility-shifted band, consistent with a single phosphorylated site during normal cell cycle progression. To identify this phosphorylation site, Jurkat clones expressing WT, S70A, or S87A BCL-2 were elutriated, and cell cycle-enriched fractions were analyzed. One discrete mobility-shifted band was observed in the $G_2$/M fraction of WT and S87A clones but not in the S70A clone, demonstrating that Ser70 is the major phosphorylation site in cycling cells (Fig. 4B).

To determine if cells vary in susceptibility to apoptosis throughout the cell cycle, the elutriated fractions were treated with anti-Fas Ab, and cell viability was determined. The $G_2$/M-enriched cells expressing WT BCL-2 demonstrated an increased vulnerability to cell death (~155%) compared to the asynchronous population (considered the control and denoted as 100% relative cell death) (Fig. 4C). Evidence that this increased susceptibility at $G_2$/M was attributable to the phosphorylation of BCL-2 was provided by the Jurkat clone expressing BCL-2 S70A. The presence of BCL-2 S70A restored resistance to the $G_2$/M fraction of cells to an anti-Fas Ab stimulus (Fig. 4C).

**Cyclin B1-Cdc2 is not a BCL-2 kinase.** These findings suggest that endogenous BCL-2 is phosphorylated by a kinase activated at $G_2$/M. An obvious candidate would be Cdc2, although the BCL-2 phosphorylation sites S70 and S87 only weakly match the phosphorylation consensus site for Cdc2 substrates (S/T-P-X-R>S/T-P) (40). To test this possibility, cellular lysates from elutriation-enriched $G_1$, S, or $G_2$/M fractions of Jurkat cells were immunoprecipitated with anti-cyclin B1 Ab, and an in vitro kinase assay was performed by using recombinant BCL-2-His or histone H1 as the substrate. Cdc2, as expected, was activated at $G_2$/M and phosphorylated its classic substrate histone H1 but did not phosphorylate BCL-2 (Fig. 5A). This indicates Cdc2 is not the responsible kinase even though it has been shown to be activated by paclitaxel and participates in the apoptosis of breast cancer cells (68).

To gain information about the BCL-2 kinase, we tested a series of kinase inhibitors to determine if they affected BCL-2 phosphorylation. Jurkat-BCL-2 cells were pretreated with various kinase inhibitors and subsequently exposed to paclitaxel (Fig. 5B). Staurosporine (a broad-spectrum Ser/Thr kinase inhibitor) and genistein (a Tyr kinase inhibitor) each markedly inhibited paclitaxel-induced BCL-2 phosphorylation. In contrast, phosphatidylinositol 3-kinase inhibitors (wortmannin and LY 294002), a MEK inhibitor (PD98059), p38 inhibitors (SB203580 and SB202190), a p70 S6 kinase inhibitor (rapamycin), and a PKA inhibitor (Rp-cAMP) did not substantially impair BCL-2 phosphorylation. Thus, this inhibitor study implicates both protein tyrosine kinase(s) and Ser/Thr kinase(s) in paclitaxel-induced BCL-2 phosphorylation.

**ASK1 and JNK1 are activated at $G_2$/M, and JNK1 phosphorylates BCL-2.** BCL-2 phosphorylation sites conform to the

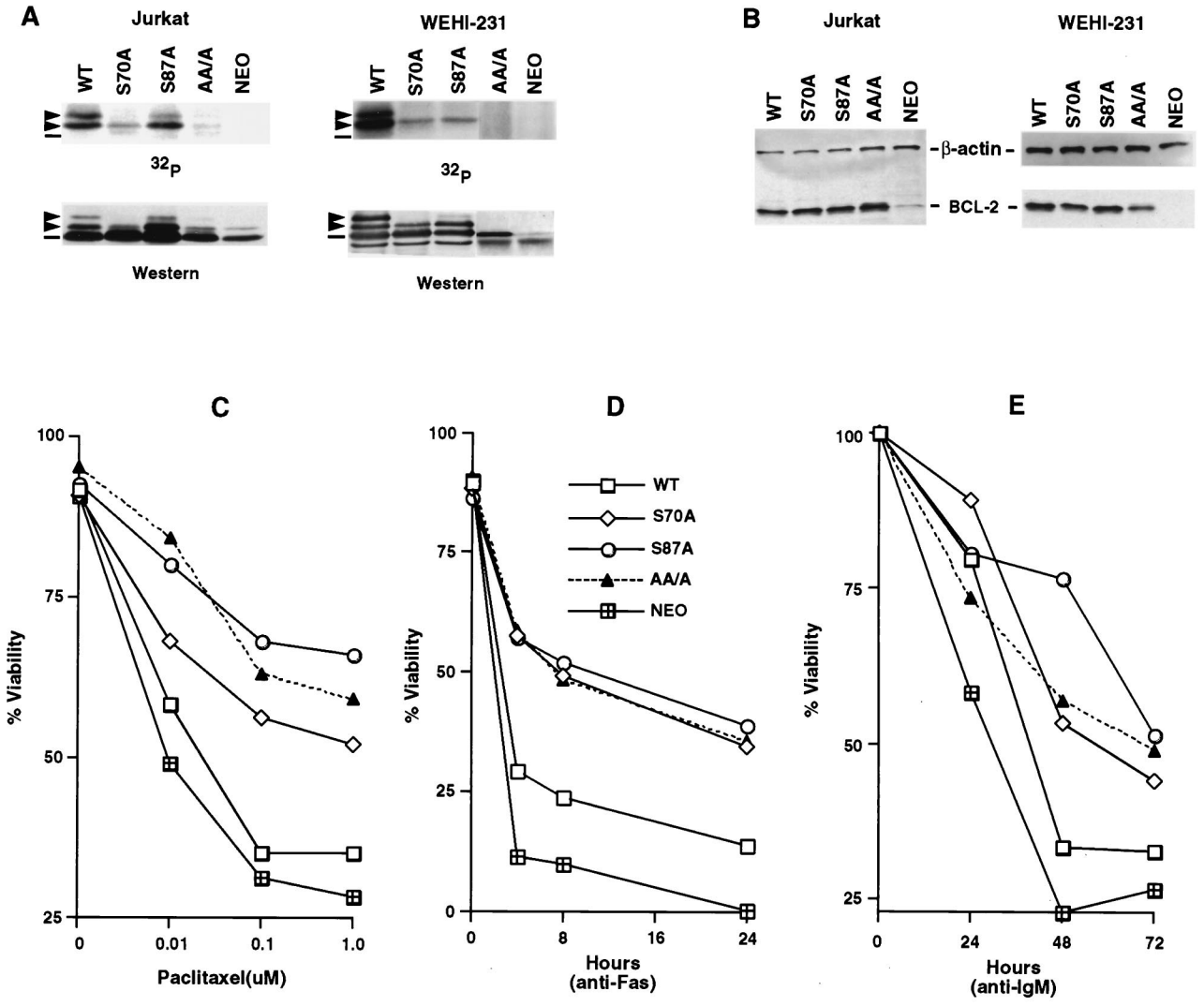


FIG. 3. Substitution of phosphorylation sites in BCL-2 further enhances antiapoptotic activity. (A) Jurkat clones and WEHI-231 clones stably expressing WT or alanine-substituted phosphorylation sites of BCL-2, consisting of Ser70 (S70A), Ser87 (S87A), or all three phosphorylation sites, including Thr69 plus the two serines (AA/A), or an empty vector (Neo) were generated. Cells were treated with 1 μM paclitaxel for Jurkat clones or 1 μM vincristine for WEHI-231 clones and in vivo labeled with $^{32}$P-orthophosphate. BCL-2 was immunoprecipitated, separated by SDS-PAGE, and transferred to a membrane. After autoradiography, the same membranes were used for immunoblotting. Arrowheads denote phosphorylated BCL-2, and dashes denote nonphosphorylated BCL-2. The residual-shifted band on Western analysis of Jurkat cells bearing AA/A or Neo represents the endogenous hBCL-2 of Jurkat cells. (B) BCL-2 expression levels in Jurkat and WEHI-231 clones, determined by Western blot analysis of lysates from equivalent cells of various Jurkat or WEHI-231 clones with anti-hBCL-2 Ab 6C8 and anti-β-actin Ab. (C to E) Cell viability assays of Jurkat clones (C and D) or WEHI-231 clones (E). Jurkat clones expressing comparable WT, S70A, S87A, AA/A BCL-2, or Neo control vector were stimulated with various doses of paclitaxel for 24 h (C) or anti-Fas antibody (100 ng/ml) (D), while WEHI-231 clones were treated with anti-IgM Ab (BET-2 supernatant at 1:100 dilution) (E). Viability was determined by PI exclusion using flow cytometry. The results represent the means of triplicate assays. Another independent set of clones expressing matched levels of WT or mutant BCL-2 showed comparable results.

consensus motif for substrates of MAP kinase and JNK/SAPK, yet the lack of response to kinase inhibitors (PD98059, SB203580, and SB202190) suggests that ERKs and p38 are not likely to be the BCL-2 kinase. Paclitaxel has been shown to result in JNK/SAPK activation (64). Its candidacy was supported by an immune complex kinase assay performed with endogenous JNK immunoprecipitated from Jurkat cells treated with anisomycin (10 μg/ml) or UV (300 J/m$^2$) for 30 min. The immunoprecipitated, activated JNK phosphorylated recombinant BCL-2-His as well as its standard substrate GST–c-Jun (data not shown). Since BCL-2 was phosphorylated at $G_2$/M in normally cycling cells, we next tested whether JNK was activated at $G_2$/M and capable of phosphorylating BCL-2. JNK was immunoprecipitated from the cell cycle-enriched fractions of elutriated Jurkat cells and subjected to in vitro kinase assays. JNK from the $G_2$/M fraction was threefold more active than at $G_1$, as assayed with c-Jun as a substrate, and also proved more potent for phosphorylating recombinant BCL-2.

ASK1 is a member of the MAP3K (MAP kinase kinase kinase) subfamily which activates the JNK pathway and is required for tumor necrosis factor- and Fas-Daxx-induced apoptosis (6, 25). ASK1 has also been noted to be activated by microtubule-damaging agents (64). Consequently, we examined ASK1 activity within the cell cycle fractions of Jurkat cells. ASK1 activity was approximately sixfold higher at $G_2$/M than at the $G_1$ phase (Fig. 5C).

**An ASK1/MKK7/JNK1 pathway is responsible for the phosphorylation of BCL-2 in vivo.** To determine whether the

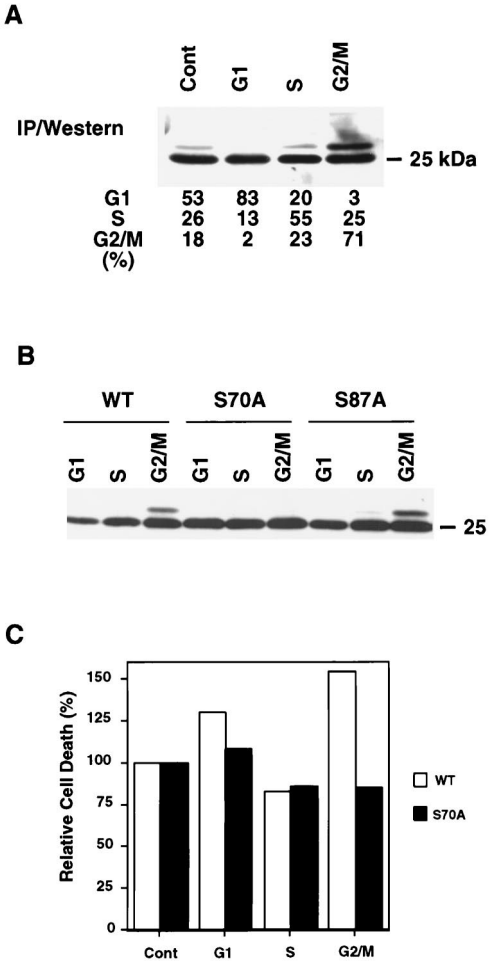


FIG. 4. Phosphorylation of BCL-2 during the cell cycle. (A) Phosphorylation of endogenous BCL-2 at $G_2$/M phase. Jurkat-Neo cells were elutriated to enrich for $G_1$, S, and $G_2$/M fractions and compared to asynchronous cells (Cont). Cellular lysates were subjected to immunoprecipitation (IP) with anti-BCL-2 monoclonal Ab 6C8 and the subsequent Western blot was developed with anti-hBCL-2 Ab Bcl-2/100. The percentages of cells in $G_1$, S, and $G_2$/M were determined by PI staining using FACScan and CELLQUEST software. (B) Ser70 was phosphorylated in cycling cells. Jurkat clones expressing WT, S70A, or S87A BCL-2 were elutriated and subjected to Western analysis. (C) Cells with phosphorylated BCL-2 at $G_2$/M demonstrated increased susceptibility to apoptosis. Jurkat clones expressing WT or S70A BCL-2 were elutriated, and typical $G_1$-, S-, and $G_2$/M-enriched fractions were compared to asynchronous cells (Cont). Cells were treated with 100 ng of anti-Fas Ab per ml, and cell viability was determined by PI exclusion 6 h later. Values represent the relative viability of each fraction when the viability of the asynchronous cells is set at 100%. Values are the means of duplicate assays.

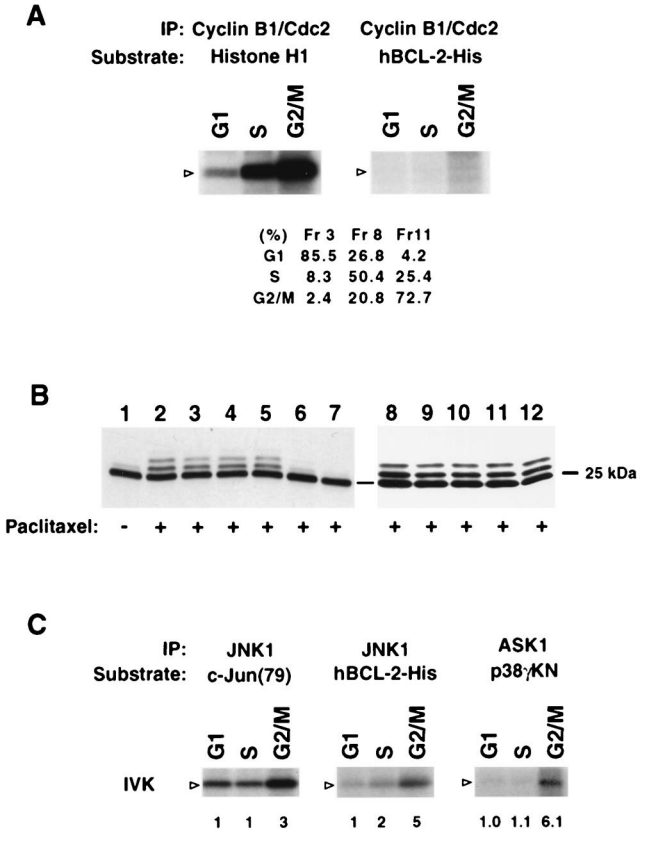


FIG. 5. $G_2$/M-activated ASK1-JNK1 pathway and JNK1 phosphorylation of BCL-2 in vitro. (A) $G_2$/M-activated cyclin B1-Cdc2 complex does not phosphorylate BCL-2. Elutriated $G_1$ (fraction [Fr] 3), S (Fr 8), and $G_2$/M (Fr 11) fractions of Jurkat cells were lysed and immunoprecipitated (IP) with anti-cyclin B1. The phosphorylation of substrate histone H1 was assessed. The activity of this kinase complex for recombinant hBCL-2-His was also assessed. Arrowheads denote the position of the substrate. Cell cycle status was assayed by PI staining using a FACScan and CELLQUEST software. (B) Genistein and staurosporine inhibit paclitaxel-induced BCL-2 phosphorylation. Jurkat cells expressing WT BCL-2 were pretreated with various kinase inhibitors including 50 μM PD98059 (lane 3), 10 μM SB203580 (lane 4), 10 μM SB202190 (lane 5), 10 μg of genistein per ml (lane 6), 0.1 μM staurosporine (lane 7), 100 μM Rp-cAMP (lane 9), 10 μM LY294002 (lane 10), 1 μM wortmannin (lane 11), 20 ng of rapamycin per ml (lane 12), or DMSO (lanes 1, 2, and 8) for 60 min and then treated with (+) or without (−) paclitaxel for 6 h. BCL-2 phosphorylation was examined by Western blot analysis. (C) In vitro kinase (IVK) assay. The ASK1-JNK1 pathway is activated at the $G_2$/M stage in cycling cells, and JNK1 phosphorylates BCL-2 in vitro. Lysates from elutriated fractions of Jurkat cells were immunoprecipitated with anti-ASK1 (DAV) serum or anti-JNK1 antibody. The ASK1 complex was incubated with GST-MKK6 and then with GST-p38γKN as a substrate to measure kinase activity. JNK activity was determined with GST–c-Jun (79) as a substrate. Recombinant hBCL-2-His was also incubated with the JNK1 complex. The position of substrates is denoted by open arrowheads. The fold activation of kinase activity is indicated as detected by phosphorimage analysis with activity at $G_1$ set at 1.0. Western analysis of immunoprecipitates confirmed an equivalent amount of the kinase protein in each fraction (not shown).

ASK1-JNK pathway phosphorylated BCL-2 in vivo, we cotransfected 293 cells with an expression vector for BCL-2 together with an ASK1 vector and/or increasing amounts of a JNK1 vector. BCL-2 phosphorylation was induced by JNK1 in a dose-dependent manner but was dependent on the presence of ASK1 (Fig. 6A). The activation of exogenous JNK1 was confirmed by an anti-phospho-JNK-specific Ab (Fig. 6A). Transfection of ASK1 alone resulted in modest phosphorylation of BCL-2 mediated by activation of endogenous JNK (Fig. 6A). In contrast, p38 kinase with or without ASK1 cotransfection was not nearly as effective at phosphorylating BCL-2 (Fig. 6A), consistent with the kinase inhibitor data (Fig. 5B).

The accuracy of transfected ASK1/JNK1 in phosphorylating the correct sites of BCL-2 was examined by comparing cotransfections of mutant and WT BCL-2. ASK1/JNK1 resulted in two mobility-shifted bands of WT BCL-2, suggesting single and double phosphorylation of Ser70 and Ser87 (Fig. 6B). Consistent with this, the single-site mutants (S70A and S87A) revealed a single-shifted moiety. The lack of any mobility shift for the double (S70A S87A) or triple AA/A (T69A S70A S87A) mutants confirmed that ASK1/JNK1 phosphorylates the relevant BCL-2 sites normally phosphorylated at $G_2$/M or by paclitaxel treatment.

To assess whether the endogenous ASK1/JNK1 pathway is responsible for BCL-2 phosphorylation, we used dominant-negative versions of kinases within this pathway (Fig. 6C). No

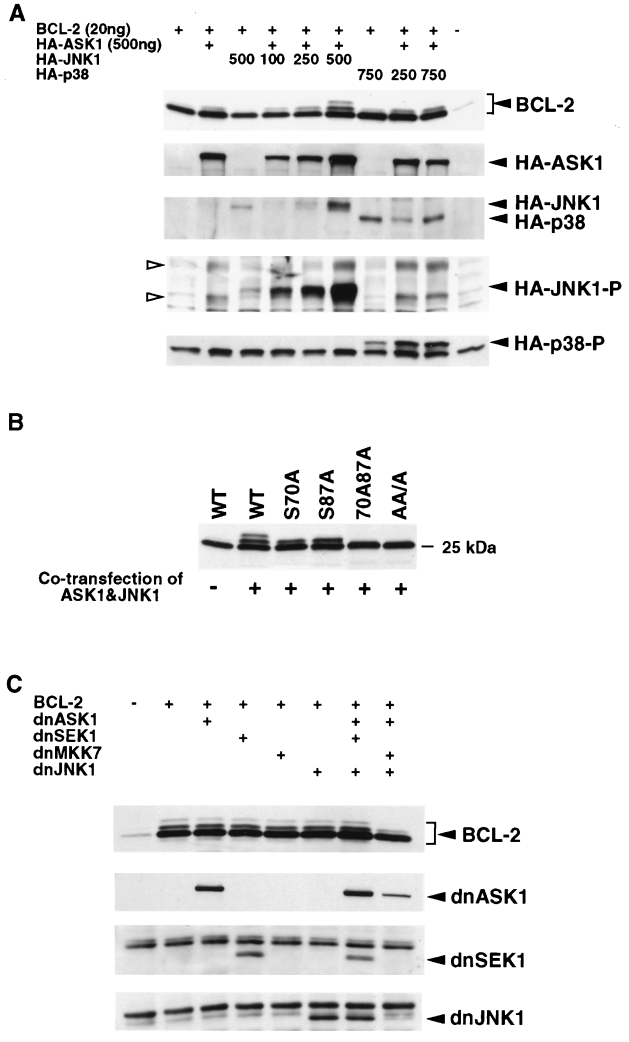


FIG. 6. ASK1-JNK1 pathway phosphorylates BCL-2 in vivo. (A) Dose-dependent phosphorylation of BCL-2 by JNK1 in vivo. 293 cells were transfected with 20 ng of hBCL-2 or control vector together with indicated amounts of HA-ASK1, HA-JNK1, and/or HA-p38, as shown. The total amount of transfected DNA was kept constant by adding a compensating amount of empty vector pcDNA3. After 24 h, cells were lysed and the phosphorylation of BCL-2, expression level of each kinase, and activation of JNK and p38 were determined by Western analysis. Open arrowheads denote the activated endogenous JNKs (p46 and p54). (B) Substrate specificity of ASK1-JNK1 pathway in vivo. WT or phosphorylation site mutant BCL-2 expression vectors (20 ng) were cotransfected with ASK1 (500 ng) and JNK (750 ng) or pcDNA3 into 293 cells. Lysates generated 24 h after transfection were assessed for BCL-2 phosphorylation by Western analysis. (C) Inhibition of BCL-2 phosphorylation by dnASK1, dnMKK7, and dnJNK1. WT BCL-2 (20 ng) was cotransfected with dnASK1 (500 ng), dnSEK1 (500 ng), dnMKK7 (500 ng), and dnJNK1 (750 ng), as indicated, into 293 cells. The total amount of DNA transfected was normalized by adding pcDNA3. After 16 h, paclitaxel was added to a final concentration of 1 μM and cells were incubated an additional 8 h. BCL-2 phosphorylation and the expression levels of the dominant-negative (dn) kinases were determined by immunoblotting.

single dominant-negative kinase expression vector was capable of inhibiting paclitaxel-induced phosphorylation of BCL-2. However, inhibition of multiple steps in the pathway by cotransfection of dnASK1, dnMKK7, and dnJNK1 together markedly inhibited BCL-2 phosphorylation. Of note, dnSEK1 was not as effective as dnMKK7 (Fig. 6C). These data support an ASK1/MKK7/JNK1 axis in the phosphorylation of BCL-2.

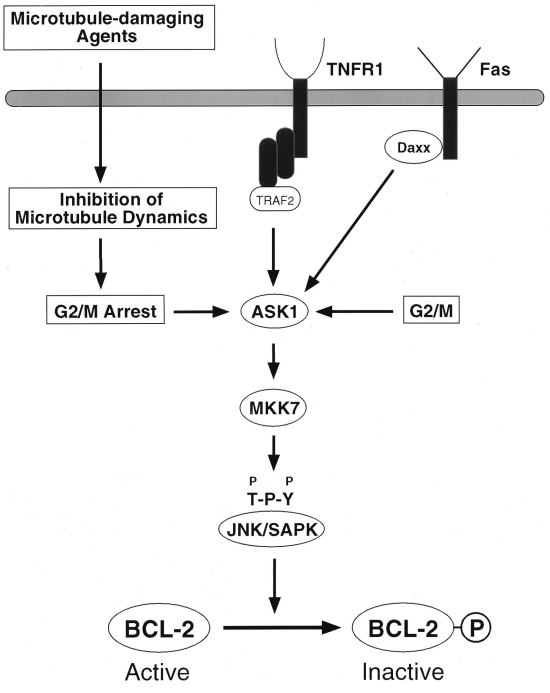


FIG. 7. Schematic representation of the ASK1/MKK7/JNK1 pathway in BCL-2 phosphorylation. ASK1, a MAP3K, is activated by extracellular and intracellular stimuli to induce JNK pathway activation. JNK phosphorylates BCL-2, inactivating its antiapoptotic function. TNFR1, tumor necrosis factor receptor 1.

## DISCUSSION

The phosphorylation of BCL-2 is a further example of how posttranslational modifications can interconvert active to inactive conformations of BCL-2 family molecules. However, uncertainty existed in the literature as to whether this phosphorylation activates (36) or inactivates (21) the antiapoptotic function of BCL-2. Consequently, we elected to first perform detailed 2D mapping and sequence identification of the in vivo phosphorylation sites on BCL-2 followed by their individual and collective substitution. Ser70, Ser87, and Thr69 proved to be phosphorylated, and all are located within the unstructured loop region between the α1 and α2 helices of BCL-2. The three mobility-shifted bands correspond to one, two, or three sites of phosphorylation, respectively. The number of phosphorylated sites appears to depend on the intensity of kinase activation. During normal cell cycle progression, Ser70 is the principal phosphorylation site. Haldar et al. (19) and Srivastava et al. (55) also noted Ser70 as the major site of phosphorylation in response to microtubule-damaging agents. We have also noted that following paclitaxel, Ser70 is phosphorylated before Ser87 (not shown) although this sequence of events is not obligate, as Ser87 is phosphorylated in an S70A mutant. The single S70A and S87A mutants and the triple AA/A mutant all demonstrate augmented antideath activity due to microtubule damage by paclitaxel or vincristine or to the physiologic anti-IgM or anti-Fas Ab signals. This evidence that BCL-2 phosphorylation is inactivating is in keeping with the observation that phosphorylated BCL-2 is less likely to heterodimerize with BAX molecules (47, 55). This is consistent with the initial proposal that the phosphorylation of BCL-2 would be inactivating (20). Our findings disagree with observations on a different system in which an S70A BCL-2 mutant displays less protection in NSF/N1.H7 cells, an IL-3-dependent cell line (27), although we

found that the S70A mutant was capable of protecting another IL-3-dependent line, FL5.12 (44a). Of note, all BCL-2 mutants studied here (S70A, S87A, and the triple AA/A) demonstrate roughly comparable protection, which suggests that the three sites might act in concert to regulate BCL-2. Of interest, the protection offered by these mutants, including BCL-2 AA/A, which eliminates all phosphorylation, was not as complete as that reported for mutants lacking the unstructured loop (5, 54). While this might suggest modifications to the loop beyond phosphorylation, it is also conceivable that the loop deletion more effectively locks BCL-2 in an active conformation whereas phosphorylation only influences an equilibrium between active and inactive conformers.

The phosphorylation of BCL-2 at the $G_2$/M phase of normally cycling cells indicates that the phosphorylation of BCL-2 is a normal physiologic process rather than exclusively a response to microtubule damage. The capacity of drugs with multiple actions, including nocodazole, taxanes and vinca alkaloids, to all result in BCL-2 phosphorylation suggests that arrest at $G_2$/M might be the common event. What would be the purpose of inactivating BCL-2 at $G_2$/M? Prior evidence of an interrelationship between cell cycle progression and BCL-2 exists. In IL-3-dependent cells, the phosphorylation of BCL-2 was temporally correlated with entry into the cell cycle (47). *Bcl-2*-deficient T cells demonstrated accelerated cell cycle entry but at the risk of increased apoptosis. In contrast, overexpression of BCL-2 delays entry into S phase and in T cells apparently at the restriction point, reflected by diminished IL-2 production upon activation (31, 37, 45, 61). If BCL-2 had a similar arresting affect at $G_2$/M, phosphorylation might be required for its release. Alternatively, evidence presented here supports another model: that cells are more susceptible to a death signal during $G_2$/M and that characteristic can be attributed to phosphorylation of BCL-2. Thus, a rationale for lowering the threshold for apoptosis at $G_2$/M would be to ensure the elimination of cells with aberrations of chromosomal segregation. In support of this model, overexpression of BCL-$X_L$ has been noted to result in increased tetraploidization (39).

Our finding indicated that the same ASK1/JNK pathway is responsible for the normal cell cycle-related and paclitaxel-induced phosphorylation of BCL-2 (Fig. 7). This suggests that the phosphorylation of BCL-2 in response to the microtubule-damaging drugs could simply be an exaggerated normal process secondary to their $G_2$/M arrest. Alternatively, a more intimate relationship could exist in that the same agents (taxanes, vinca alkaloids, nocodazole, and colchicine) that result in the phosphorylation of BCL-2 also activate the ASK1/JNK kinase pathway (64). In our examination, no single dominant negative kinase in this pathway was capable of blocking paclitaxel-induced phosphorylation of BCL-2, consistent with other observations (63). However, combined dominant negatives for each step of the pathway (dnASK1/dnMKK7/dnJNK1) interfered quite effectively with BCL-2 phosphorylation. Consistent with this, the combined overexpression of WT ASK1/JNK1 was capable of phosphorylating BCL-2 in vivo. The JNK family has been reported to mediate both proapoptotic and antiapoptotic responses, perhaps reflecting cell type specificity (26). This is supported by *Jnk1*/*Jnk2* double-deficient embryos, which revealed region-specific apoptosis with reduced death in the hindbrain but increased apoptosis in the forebrain (29). Neither SEK1 nor p38 had obvious effects despite the fact that p38 is implicated as a component of the mitotic spindle checkpoint (59). Recently, activated JNK1/2 has been shown to colocalize with a MAP3K, MLK (mixed lineage) Ser/Thr kinase, to punctate structures along microtubules. Of potential interest, MLK interacts with the KIF3 family of kinesin motor proteins (42). In further support of a direct relationship between microtubules and the cell death pathway, another BCL-2 family member BIM binds to the LC8 dynein light-chain protein (48). In this context, organelles including mitochondria are transported along microtubules by means of microtubule-associated motor proteins (23). BCL-2 localizes to mitochondria, endoplasmic reticulum, and nuclear envelope, and transportation along microtubules arranges these organelles on a metaphase plate to allow equal segregation of them to daughter cells at mitosis. Thus, BCL-2 associated with these organelles could be placed in apposition with activated JNK pathway kinases found at microtubules. Thus, drugs which cause microtubule dysfunction would be activating the same MAP3K/JNK pathway, prompting the phosphorylation of a normal substrate(s) including BCL-2 (Fig. 7).

## ACKNOWLEDGMENTS

We are grateful to R. J. Davis, S. Gutkind, G. L. Johnson, J. Kyriakis, E. Nishida, and H. Saito for providing the expression vectors described above and to Steven F. Dowdy, David S. Pellman, Mark Dalton, and Zoltan Oltvai for technical advice and scientific discussion. We also thank Deborah S. Maher for secretarial assistance.

K.Y. was a fellow of the National Cancer Institute (U.S.A.)-Japanese Foundation for Cancer Research Research Training Program and is supported in part by the Uehara Memorial Foundation Research Fellowship.

## REFERENCES

1. **Bakhshi, A., J. P. Jensen, P. Goldman, J. J. Wright, O. W. McBride, A. L. Epstein, and S. J. Korsmeyer.** 1985. Cloning the chromosomal breakpoint of t(14;18) human lymphomas: clustering around JH on chromosome 14 and near a transcriptional unit on 18. Cell **41:**899–906.
2. **Blagosklonny, M. V., P. Giannakakou, W. S. el-Deiry, D. G. Kingston, P. I. Higgs, L. Neckers, and T. Fojo.** 1997. Raf-1/bcl-2 phosphorylation: a step from microtubule damage to cell death. Cancer Res. **57:**130–135.
3. **Blume-Jensen, P., R. Janknecht, and T. Hunter.** 1998. The kit receptor promotes cell survival via activation of PI 3-kinase and subsequent Akt-mediated phosphorylation of Bad on Ser136. Curr. Biol. **8:**779–782.
4. **Boyle, W. J., P. van der Geer, and T. Hunter.** 1991. Phosphopeptide mapping and phosphoamino acid analysis by two-dimensional separation on thin-layer cellulose plates. Methods Enzymol. **201:**110–149.
5. **Chang, B. S., A. J. Minn, S. W. Muchmore, S. W. Fesik, and C. B. Thompson.** 1997. Identification of a novel regulatory domain in Bcl-X(L) and Bcl-2. EMBO J. **16:**968–977.
6. **Chang, H. Y., H. Nishitoh, X. Yang, H. Ichijo, and D. Baltimore.** 1998. Activation of apoptosis signal-regulating kinase 1 (ASK1) by the adapter protein Daxx. Science **281:**1860–1863.
7. **Chou, J. J., H. Li, G. S. Salvesen, J. Yuan, and G. Wagner.** 1999. Solution structure of BID, an intracellular amplifier of apoptotic signaling. Cell **96:**615–624.
8. **Cleary, M. L., and J. Sklar.** 1985. Nucleotide sequence of a t(14;18) chromosomal breakpoint in follicular lymphoma and demonstration of a breakpoint-cluster region near a transcriptionally active locus on chromosome 18. Proc. Natl. Acad. Sci. USA **82:**7439–7443.
9. **Coso, O. A., M. Chiariello, J. C. Yu, H. Teramoto, P. Crespo, N. Xu, T. Miki, and J. S. Gutkind.** 1995. The small GTP-binding proteins Rac1 and Cdc42 regulate the activity of the JNK/SAPK signaling pathway. Cell **81:**1137–1146.
10. **Cryns, V., and J. Yuan.** 1998. Proteases to die for. Genes Dev. **12:**1551–1570.
11. **Datta, S. R., H. Dudek, X. Tao, S. Masters, H. Fu, Y. Gotoh, and M. E. Greenberg.** 1997. Akt phosphorylation of BAD couples survival signals to the cell-intrinsic death machinery. Cell **91:**231–241.
12. **del Peso, L., M. Gonzalez-Garcia, C. Page, R. Herrera, and G. Nunez.** 1997. Interleukin-3-induced phosphorylation of BAD through the protein kinase Akt. Science **278:**687–689.
13. **Derijard, B., J. Raingeaud, T. Barrett, I. H. Wu, J. Han, R. J. Ulevitch, and R. J. Davis.** 1995. Independent human MAP-kinase signal transduction pathways defined by MEK and MKK isoforms. Science **267:**682–685.
14. **Ellis, R. E., J. Y. Yuan, and H. R. Horvitz.** 1991. Mechanisms and functions of cell death. Annu. Rev. Cell Biol. **7:**663–698.
15. **Fang, G., B. S. Chang, C. N. Kim, C. Perkins, C. B. Thompson, and K. N. Bhalla.** 1998. "Loop" domain is necessary for taxol-induced mobility shift and phosphorylation of Bcl-2 as well as for inhibiting taxol-induced cytosolic accumulation of cytochrome c and apoptosis. Cancer Res. **58:**3202–3208.
16. **Green, D. R., and J. C. Reed.** 1998. Mitochondria and apoptosis. Science **281:**1309–1312.
17. **Gross, A., J. Jockel, M. C. Wei, and S. J. Korsmeyer.** 1998. Enforced dimerization of BAX results in its translocation, mitochondrial dysfunction and apoptosis. EMBO J. **17:**3878–3885.

18. **Gross, A., X. M. Yin, K. Wang, M. C. Wei, J. Jockel, C. Milliman, H. Erdjument-Bromage, P. Tempst, and S. J. Korsmeyer.** 1999. Caspase cleaved BID targets mitochondria and is required for cytochrome c release, while BCL-XL prevents this release but not tumor necrosis factor-R1/Fas death. J. Biol. Chem. **274:**1156–1163.
19. **Haldar, S., A. Basu, and C. M. Croce.** 1998. Serine-70 is one of the critical sites for drug-induced Bcl2 phosphorylation in cancer cells. Cancer Res. **58:**1609–1615.
20. **Haldar, S., J. Chintapalli, and C. M. Croce.** 1996. Taxol induces bcl-2 phosphorylation and death of prostate cancer cells. Cancer Res. **56:**1253–1255.
21. **Haldar, S., N. Jena, and C. M. Croce.** 1995. Inactivation of Bcl-2 by phosphorylation. Proc. Natl. Acad. Sci. USA **92:**4507–4511.
22. **Harada, H., B. Becknell, M. Wilm, M. Mann, L. J. Huang, S. S. Taylor, J. D. Scott, and S. J. Korsmeyer.** 1999. Phosphorylation and inactivation of BAD by mitochondria-anchored protein kinase A. Mol. Cell **3:**413–422.
23. **Hirokawa, N.** 1998. Kinesin and dynein superfamily proteins and the mechanism of organelle transport. Science **279:**519–526.
24. **Hsu, Y. T., K. G. Wolter, and R. J. Youle.** 1997. Cytosol-to-membrane redistribution of Bax and Bcl-X(L) during apoptosis. Proc. Natl. Acad. Sci. USA **94:**3668–3672.
25. **Ichijo, H., E. Nishida, K. Irie, P. ten Dijke, M. Saitoh, T. Moriguchi, M. Takagi, K. Matsumoto, K. Miyazono, and Y. Gotoh.** 1997. Induction of apoptosis by ASK1, a mammalian MAPKKK that activates SAPK/JNK and p38 signaling pathways. Science **275:**90–94.
26. **Ip, Y. T., and R. J. Davis.** 1998. Signal transduction by the c-Jun N-terminal kinase (JNK)—from inflammation to development. Curr. Opin. Cell Biol. **10:**205–219.
27. **Ito, T., X. Deng, B. Carr, and W. S. May.** 1997. Bcl-2 phosphorylation required for anti-apoptosis function. J. Biol. Chem. **272:**11671–11673.
28. **Johnson, N. L., A. M. Gardner, K. M. Diener, C. A. Lange-Carter, J. Gleavy, M. B. Jarpe, A. Minden, M. Karin, L. I. Zon, and G. L. Johnson.** 1996. Signal transduction pathways regulated by mitogen-activated/extracellular response kinase kinase kinase induce cell death. J. Biol. Chem. **271:**3229–3237.
29. **Kuan, C. Y., D. D. Yang, D. R. Samanta Roy, R. J. Davis, P. Rakic, and R. A. Flavell.** 1999. The Jnk1 and Jnk2 protein kinases are required for regional specific apoptosis during early brain development. Neuron **22:**667–676.
30. **Li, H., H. Zhu, C. J. Xu, and J. Yuan.** 1998. Cleavage of BID by caspase 8 mediates the mitochondrial damage in the Fas pathway of apoptosis. Cell **94:**491–501.
31. **Linette, G. P., Y. Li, K. Roth, and S. J. Korsmeyer.** 1996. Cross talk between cell death and cell cycle progression: BCL-2 regulates NFAT-mediated activation. Proc. Natl. Acad. Sci. USA **93:**9545–9552.
32. **Ling, Y. H., C. Tornos, and R. Perez-Soler.** 1998. Phosphorylation of Bcl-2 is a marker of M phase events and not a determinant of apoptosis. J. Biol. Chem. **273:**18984–18991.
33. **Lissy, N. A., L. F. Van Dyk, M. Becker-Hapak, A. Vocero-Akbani, J. H. Mendler, and S. F. Dowdy.** 1998. TCR antigen-induced cell death occurs from a late G1 phase cell cycle check point. Immunity **8:**57–65.
34. **Luo, X., I. Budihardjo, H. Zou, C. Slaughter, and X. Wang.** 1998. Bid, a Bcl2 interacting protein, mediates cytochrome c release from mitochondria in response to activation of cell surface death receptors. Cell **94:**481–490.
35. **Maundrell, K., B. Antonsson, E. Magnenat, M. Camps, M. Muda, C. Chabert, C. Gillieron, U. Boschert, E. Vial-Knecht, J. C. Martinou, and S. Arkinstall.** 1997. Bcl-2 undergoes phosphorylation by c-Jun N-terminal kinase/stress-activated protein kinases in the presence of the constitutively active GTP-binding protein Rac1. J. Biol. Chem. **272:**25238–25242.
36. **May, W. S., P. G. Tyler, T. Ito, D. K. Armstrong, K. A. Qatsha, and N. E. Davidson.** 1994. Interleukin-3 and bryostatin-1 mediate hyperphosphorylation of BCL2 alpha in association with suppression of apoptosis. J. Biol. Chem. **269:**26865–26870.
37. **Mazel, S., D. Burtrum, and H. T. Petrie.** 1996. Regulation of cell division cycle progression by bcl-2 expression: a potential mechanism for inhibition of programmed cell death. J. Exp. Med. **183:**2219–2226.
38. **McDonnell, J. M., D. Fushman, C. L. Milliman, S. J. Korsmeyer, and D. Cowburn.** 1999. Solution structure of the proapoptotic molecule BID: a structural basis for apoptotic agonists and antagonists. Cell **96:**625–634.
39. **Minn, A. J., L. H. Boise, and C. B. Thompson.** 1996. Expression of Bcl-xL and loss of p53 can cooperate to overcome a cell cycle checkpoint induced by mitotic spindle damage. Genes Dev. **10:**2621–2631.
40. **Moreno, S., and P. Nurse.** 1990. Substrates for p34cdc2: in vivo veritas? Cell **61:**549–551.
41. **Moriguchi, T., F. Toyoshima, N. Masuyama, H. Hanafusa, Y. Gotoh, and E. Nishida.** 1997. A novel SAPK/JNK kinase, MKK7, stimulated by TNFalpha and cellular stresses. EMBO J. **16:**7045–7053.
42. **Nagata, K., A. Puls, C. Futter, P. Aspenstrom, E. Schaefer, T. Nakata, N. Hirokawa, and A. Hall.** 1998. The MAP kinase kinase kinase MLK2 co-localizes with activated JNK along microtubules and associates with kinesin superfamily motor KIF3. EMBO J. **17:**149–158.
43. **Nishitoh, H., M. Saitoh, Y. Mochida, K. Takeda, H. Nakano, M. Rothe, K. Miyazono, and H. Ichijo.** 1998. ASK1 is essential for JNK/SAPK activation by TRAF2. Mol. Cell **2:**389–395.
44. **Oltvai, Z. N., and S. J. Korsmeyer.** 1994. Checkpoints of dueling dimers foil death wishes. Cell **79:**189–192.

44a. **Oltvai, Z. N., and S. J. Korsmeyer.** Unpublished observation.

45. **O'Reilly, L. A., D. C. Huang, and A. Strasser.** 1996. The cell death inhibitor Bcl-2 and its homologues influence control of cell cycle entry. EMBO J. **15:**6979–6990.
46. **Ottilie, S., J. L. Diaz, W. Horne, J. Chang, Y. Wang, G. Wilson, S. Chang, S. Weeks, L. C. Fritz, and T. Oltersdorf.** 1997. Dimerization properties of human BAD. Identification of a BH-3 domain and analysis of its binding to mutant BCL-2 and BCL-XL proteins. J. Biol. Chem. **272:**30866–30872.
47. **Poommipanit, P., B. Chen, and Z. N. Oltvai.** 1999. Interleukin-3 induces the phosphorylation of a distinct fraction of bcl-2. J. Biol. Chem. **274:**1033–1039.
48. **Puthalakath, H., D. C. Huang, L. A. O'Reilly, S. M. King, and A. Strasser.** 1999. The proapoptotic activity of the Bcl-2 family member Bim is regulated by interaction with the dynein motor complex. Mol. Cell **3:**287–296.
49. **Raff, M. C.** 1992. Social controls on cell survival and cell death. Nature **356:**397–400.
50. **Rana, A., K. Gallo, P. Godowski, S. Hirai, S. Ohno, L. Zon, J. M. Kyriakis, and J. Avruch.** 1996. The mixed lineage kinase SPRK phosphorylates and activates the stress-activated protein kinase activator, SEK-1. J. Biol. Chem. **271:**19025–19028.
51. **Rodi, D. J., R. W. Janes, H. J. Sanganee, R. A. Holton, B. A. Wallace, and L. Makowski.** 1999. Screening of a library of phage-displayed peptides identifies human bcl-2 as a taxol-binding protein. J. Mol. Biol. **285:**197–203.
52. **Ruvolo, P. P., X. Deng, B. K. Carr, and W. S. May.** 1998. A functional role for mitochondrial protein kinase Calpha in Bcl2 phosphorylation and suppression of apoptosis. J. Biol. Chem. **273:**25436–25442.
53. **Scatena, C. D., Z. A. Stewart, D. Mays, L. J. Tang, C. J. Keefer, S. D. Leach, and J. A. Pietenpol.** 1998. Mitotic phosphorylation of Bcl-2 during normal cell cycle progression and Taxol-induced growth arrest. J. Biol. Chem. **273:**30777–30784.
54. **Srivastava, R. K., Q. S. Mi, J. M. Hardwick, and D. L. Longo.** 1999. Deletion of the loop region of Bcl-2 completely blocks paclitaxel-induced apoptosis. Proc. Natl. Acad. Sci. USA **96:**3775–3780.
55. **Srivastava, R. K., A. R. Srivastava, S. J. Korsmeyer, M. Nesterova, Y. S. Cho-Chung, and D. L. Longo.** 1998. Involvement of microtubules in the regulation of Bcl2 phosphorylation and apoptosis through cyclic AMP-dependent protein kinase. Mol. Cell. Biol. **18:**3509–3517.
56. **Steller, H.** 1995. Mechanisms and genes of cellular suicide. Science **267:**1445–1449.
57. **Sullivan, S., and T. W. Wong.** 1991. A manual sequencing method for identification of phosphorylated amino acids in phosphopeptides. Anal. Biochem. **197:**65–68.
58. **Takekawa, M., and H. Saito.** 1998. A family of stress-inducible GADD45-like proteins mediate activation of the stress-responsive MTK1/MEKK4 MAPKKK. Cell **95:**521–530.
59. **Takenaka, K., T. Moriguchi, and E. Nishida.** 1998. Activation of the protein kinase p38 in the spindle assembly checkpoint and mitotic arrest. Science **280:**599–602.
60. **Tsujimoto, Y., J. Cossman, E. Jaffe, and C. M. Croce.** 1985. Involvement of the bcl-2 gene in human follicular lymphoma. Science **228:**1440–1443.
61. **Vairo, G., K. M. Innes, and J. M. Adams.** 1996. Bcl-2 has a cell cycle inhibitory function separable from its enhancement of cell survival. Oncogene **13:**1511–1519.
62. **Vaux, D. L., and S. J. Korsmeyer.** 1999. Cell death in development. Cell **96:**245–254.
63. **Wang, T. H., D. M. Popp, H. S. Wang, M. Saitoh, J. G. Mural, D. C. Henley, H. Ichijo, and J. Wimalasena.** 1999. Microtubule dysfunction induced by paclitaxel initiates apoptosis through both c-Jun N-terminal kinase (JNK)-dependent and -independent pathways in ovarian cancer cells. J. Biol. Chem. **274:**8208–8216.
64. **Wang, T. H., H. S. Wang, H. Ichijo, P. Giannakakou, J. S. Foster, T. Fojo, and J. Wimalasena.** 1998. Microtubule-interfering agents activate c-Jun N-terminal kinase/stress-activated protein kinase through both Ras and apoptosis signal-regulating kinase pathways. J. Biol. Chem. **273:**4928–4936.
65. **White, E.** 1996. Life, death, and the pursuit of apoptosis. Genes Dev. **10:**1–15.
66. **Wolter, K. G., Y. T. Hsu, C. L. Smith, A. Nechushtan, X. G. Xi, and R. J. Youle.** 1997. Movement of Bax from the cytosol to mitochondria during apoptosis. J. Cell Biol. **139:**1281–1292.
67. **Yin, X. M., Z. N. Oltvai, and S. J. Korsmeyer.** 1994. BH1 and BH2 domains of Bcl-2 are required for inhibition of apoptosis and heterodimerization with Bax. Nature **369:**321–323.
68. **Yu, D., T. Jing, B. Liu, J. Yao, M. Tan, T. J. McDonnell, and M. C. Hung.** 1998. Overexpression of ErbB2 blocks Taxol-induced apoptosis by upregulation of p21Cip1, which inhibits p34Cdc2 kinase. Mol. Cell **2:**581–591.
69. **Zha, J., H. Harada, K. Osipov, J. Jockel, G. Waksman, and S. J. Korsmeyer.** 1997. BH3 domain of BAD is required for heterodimerization with BCL-XL and pro-apoptotic activity. J. Biol. Chem. **272:**24101–24104.
70. **Zha, J., H. Harada, E. Yang, J. Jockel, and S. J. Korsmeyer.** 1996. Serine phosphorylation of death agonist BAD in response to survival factor results in binding to 14-3-3 not BCL-X(L). Cell **87:**619–628.